



Design of Eutectic High Entropy Alloys in Al–Co–Cr–Fe–Ni System

Ali Shafiei¹

Received: 15 January 2020 / Accepted: 18 February 2020 / Published online: 5 March 2020
© The Korean Institute of Metals and Materials 2020

Abstract

In the present work, a simple approach is proposed for predicting the compositions of eutectic high entropy alloys (EHEAs) in Al–Co–Cr–Fe–Ni system. It is proposed that eutectic lines exist between certain eutectic alloys in this system and, as a result, new eutectic or near-eutectic compositions can be obtained by mixing the alloys which are located on the same eutectic line. The approach is applied for a series of experimentally verified eutectic alloys and new eutectic or near-eutectic alloys are designed for Al–Co–Cr–Fe–Ni system. Furthermore, by investigating the compositions of verified eutectic alloys in Al–Co–Cr–Fe–Ni system, compositional maps are proposed which show the relations between the concentrations of constituent elements in eutectic alloys. The compositional maps suggest that EHEAs are derived from binary and ternary eutectic alloys. Moreover, the proposed diagrams can be considered as convenient methods for evaluating the composition of EHEAs in Al–Co–Cr–Fe–Ni system.

Keywords High entropy alloys · High entropy eutectic alloys · Eutectic alloys

1 Introduction

High entropy alloys (HEAs) are a new group of metallic alloys which have attracted significant attentions because they could have enhanced properties in comparison with traditional alloys [1–5]. The main difference between HEAs and traditional alloys is that HEAs contain multiple (at least three) principal elements while traditional alloys are usually based on one dominant element [1–5].

A subgroup of HEAs are eutectic high entropy alloys (EHEAs) which are reported recently by Lu et al. [6]. Due to their fine in-situ lamellar composite microstructures, EHEAs have shown very promising combinations of strength and ductility [6–15] which have encouraged materials scientists to focus on EHEAs as a promising new class of structural alloys. Furthermore, these alloys may be considered as fillers for brazing due to their low melting temperatures and good viscosities. However, how easy to design EHEAs is still a challenge. That is because the phase diagrams are not available for quaternary and quinary alloy systems. In fact, most of the EHEAs were found by a trial and error approach.

Some techniques have been proposed for predicting the compositions of EHEAs [9, 14, 16–18]. One of the first methods for designing EHEAs was proposed by He et al. [9]. They noticed that similar eutectic reactions exist in Fe–Nb, Cr–Nb, Ni–Nb and Co–Nb binary systems; so, it was concluded that a eutectic alloy may also exist in pseudo-binary CoCrFeNi–Nb system. To examine this hypothesis, a series of CoCrFeNiNb_x were made and a eutectic alloy with chemical composition of CoCrFeNiNb_{0.65} was found by trial and error experiments [9]. Lu et al. introduced a grouping strategy for designing EHEAs [16]. Based on mixing enthalpies between constituent elements, it was assumed that the constituent elements of a eutectic alloy can be divided into two atomic groups [16]. Furthermore, it was proposed that the dual phase microstructure of a eutectic alloy is due to the contribution of these two atomic groups [16]. By using this hypothesis and by considering the composition of eutectic alloy AlCoCrFeNi_{2.1} as a reference, alloys Zr_{0.45}CoCrFeNi_{2.1}, Nb_{0.73}CoCrFeNi_{2.1}, Hf_{0.52}CoCrFeNi_{2.1} and Ta_{0.76}CoCrFeNi_{2.1} were designed. However, experimental results shown that these alloys were near-eutectic alloys [16]. In the next step, fully eutectic compositions of Zr_{0.6}CoCrFeNi_{2.0}, Nb_{0.74}CoCrFeNi_{2.0}, Hf_{0.55}CoCrFeNi_{2.0} and Ta_{0.65}CoCrFeNi_{2.0} were obtained by tuning the compositions using trial and error experiments [16]. Jiang et al. proposed a simple method for designing EHEAs by combining constituent binary eutectic compositions [17].

✉ Ali Shafiei
alshafiei@nri.ac.ir

¹ Metallurgy Group, Niroo Research Institute (NRI),
Tehran 14665-517, Iran

For example, alloy $\text{CoCrFeNiNb}_{0.6}$ was designed by combining binary eutectic alloys $\text{Ni}_{84.5}\text{Nb}_{15.5}$, $\text{Co}_{86.1}\text{Nb}_{13.9}$, $\text{Cr}_{88}\text{Nb}_{12}$ and $\text{Fe}_{89.4}\text{Nb}_{10.6}$ [16]. Furthermore, alloys $\text{CoCrFeNiTa}_{0.47}$, $\text{CoCrFeNiZr}_{0.51}$ and $\text{CoCrFeNiHf}_{0.49}$ were also designed [17]. But the designed alloys were determined to be near-eutectic alloys [17]. By performing few trial and error experiments, the exact eutectic compositions were determined as $\text{CoCrFeNiNb}_{0.45}$, $\text{CoCrFeNiTa}_{0.4}$, $\text{CoCrFeNiZr}_{0.55}$, and $\text{CoCrFeNiHf}_{0.4}$ [17]. Jin et al. proposed a pseudo binary strategy for designing eutectic high entropy alloys [18]. According to their strategy, EHEAs can be designed by following steps: (1) selecting appropriate stable FCC and intermetallic phases (by using parameters mixing enthalpy and valence electron concentration), (2) mixing the two phases, and then (3) adjusting the content of intermetallic forming elements with a few trial and error experiments. By using the developed model, near eutectic alloys AlCoCrFeNi_3 , $\text{AlCo}_2\text{CrFeNi}_2$, and $\text{AlCoCrFe}_2\text{Ni}_2$ were first designed, and then the exact eutectic compositions were obtained by tuning the Al and Ni content of alloys. Wu et al. used pseudo-binary CoCrNi-NiAl and pseudo-ternary NiCo-Cr-NiAl phase diagrams combined with CALPHAD calculations for predicting new EHEAs [14]. New EHEAs were designed and made, but discrepancies were observed between the CALPHAD calculations and the solidification structures of alloys [14]; exact eutectic compositions were obtained by tuning NiAl content of designed alloys.

It can be concluded that the developed approaches to design eutectic alloys can mostly predict near eutectic compositions [14, 16–18], and few trial and error experiments were needed to achieve the exact eutectic compositions [14, 16–18]. Therefore, how easy to design EHEAs is still a challenge. The objective of the present work is proposing a simple method to design EHEAs. Al–Co–Cr–Fe–Ni system is considered in this work; but it is believed that the proposed approach may also be used for other alloy systems. The approach which is proposed here is based on the compositions of verified eutectic alloys, and the assumption that eutectic lines exist between these alloys. The proposed approach do not require parameters such as atomic size difference, valence electron concentration, enthalpy of mixing, etc. for predicting the composition of eutectic alloys, although these are important parameters for qualitative predicting the constituent phases of HEAs [3–5]. Since the proposed approach do not need any empirical parameter, the proposed approach can be considered as an easy-to-use tool for designing EHEAs.

2 Methodology

2.1 Alloy Preparation and Characterization

The ingot of targeted AlCoCrFeNi alloy was prepared via arc melting the high purity constituent elements ($\text{Ni}(99.9\%$

$\text{wt}\%$), $\text{Co}(99.99\% \text{ wt}\%)$, $\text{Al}(99.999\% \text{ wt}\%)$, and $\text{Cr}(99.9\% \text{ wt}\%)$) under a Ti-gettered high purity argon atmosphere. The ingot was remelted four times to achieve compositional homogeneity. By using a water-cooled copper mold, the homogenized ingot was suction casted into a 4 cm long and 8 mm diameter rod. The sample was further sectioned perpendicular to its length for microstructural investigations which were performed by optical and scanning electron microscopes. Marble's etchant was used for the etching of the sample.

2.2 Thermodynamic Simulations

All of the simulations and thermodynamic calculations in the present work are performed by JMatPro® software version 7.0.0 developed by Sente Software Ltd.[19]. The software uses a multicomponent thermodynamic database, NiData, developed by ThermoTech Ltd.[19]. “Nickel-based superalloy” toolbox is used for the simulations. The ability of the software for modeling the solidification behaviors of various multi-component alloys is verified by several research works [20–24]. An alloy is considered as eutectic if simulation results predict that the solidification occurs in a narrow temperature range ($\Delta T_{\text{max}} = 10^\circ\text{C}$), and if during the solidification simultaneous formation of two solid phases γ (fcc) and B2 (bcc) occurs. This criterion is considered here according to the obtained simulation results for verified EHEAs [25].

3 Model Development

The chemical compositions of some of the verified binary, ternary, quaternary and quinary eutectic alloys in Al–Co–Cr–Fe–Ni system are shown in Table 1. Only binary and ternary eutectic alloys with eutectic phases γ (FCC) and B2 (BCC) are considered here. So the model which is proposed here is only valid for $\gamma + \text{B2}$ eutectic alloys. All of the reported quaternary and quinary EHEAs in Al–Co–Cr–Fe–Ni system also form phases γ and B2 during their eutectic reactions (Table 1). For ternary systems the binary eutectic reaction ($\text{L} \rightarrow \gamma + \text{B2}$) occurs along a line (Fig. 1) [26–30], therefore ranges of compositions are listed for these alloys in Table 1. The eutectic lines for ternary systems are shown in Fig. 1. The eutectic lines are in fact not entirely straight according to the ternary phase diagrams; however, for simplicity, it is assumed here that eutectic lines are straight as they are shown in Fig. 1. For Al–Co–Ni, Al–Fe–Ni and Al–Cr–Ni systems the liquidus projections are available [26–30], so eutectic lines are directly extracted from phase diagrams (Fig. 1a–c) [26–30]. However, for ternary Al–Co–Fe and Al–Co–Cr systems liquidus projections are not available. The eutectic lines for these systems

Table 1 The chemical compositions of some of the experimentally verified binary, ternary, quaternary and quinary eutectic alloys in Al–Co–Cr–Fe–Ni system

Alloys	Chemical composition (at%)					Eutectic phases
	Al	Co	Cr	Fe	Ni	
AlCo [33]	20	80	–	–	–	$\gamma + B2$
AlCoFe [31, 32]	15–20	63–80	–	0–22	–	$\gamma + B2$
AlFeNi [26]	17–22	–	–	10–50	33–68	$\gamma + B2$
AlCoNi [29, 30]	20–23	7–80	–	–	0–70	$\gamma + B2$
AlCoCr [34]	19–20	56–80	0–25	–	–	$\gamma + B2$
AlCrNi [27, 28]	17.5–23	0	4–31	0	51.5–73	$\gamma + B2$
AlCoFeNi [13]	19	20	–	20	41	$\gamma + B2$
AlCoCrNi [12]	19	15	15	–	51	$\gamma + B2$
AlCoCrNi [14]	17.4	21.7	21.7	0	39.2	$\gamma + B2$
AlCoCrNi [14]	16	38.6	22.7	0	22.7	$\gamma + B2$
AlCrFeNi ₂ [35]	16	–	20	20	44	$\gamma + B2$
AlCoCrFeNi [36]	18	30	10	10	32	$\gamma + B2$
AlCoCrFeNi _{2,1} [6]	16.4	16.4	16.4	16.4	34.4	$\gamma + B2$
AlCo ₂ CrFeNi ₂ [18]	17	28.6	14.3	14.3	25.8	$\gamma + B2$
AlCoCrFe ₂ Ni ₂ [18]	17	14.3	14.3	28.6	25.8	$\gamma + B2$
AlCoCrFeNi ₃ [18]	17	14.3	14.3	14.3	40.1	$\gamma + B2$
AlCoCrFeNi [37]	18	30	10	10	32	$\gamma + B2$
AlCoFeNi [37]	18	30	–	20	32	$\gamma + B2$
AlCoFeNi [37]	18	27.34	–	27.34	27.34	$\gamma + B2$
AlCoCrFeNi [37]*	18	30	10	10	30	$\gamma + B2$
AlCoCrFeNi [37]*	18	24	10	10	36	$\gamma + B2$
AlCoCrFeNi [37]*	18	20	10	10	40	$\gamma + B2$
AlCoCrFeNi [25]	16	41	15	10	18	$\gamma + B2$

*These alloys contained 2 at% of W for improving the mechanical properties

are obtained by following procedures. For Al–Co–Fe system the minimum eutectic composition is reported to be Al₁₅Co₆₃Fe₂₂ at% [31, 32]. Therefore, it is assumed that a straight eutectic line exists between the eutectic composition Al₂₀Co₈₀ [33] and Al₁₅Co₆₃Fe₂₂ [31, 32] (Fig. 1d). For Al–Co–Cr system neither a liquidus projection nor a minimum eutectic composition is reported. However, Liu et al. [34] modeled the isothermal section of Al–Co–Cr system at 1300 °C, and from the isothermal section, the boundaries of the two phase region $\gamma + B2$ can be obtained (Fig. 1e). According to the boundaries of the two phase region $\gamma + B2$ at 1300 °C, the eutectic line could be predicted which is shown in Fig. 1e. It should be noted that for both Al–Co–Fe and Al–Co–Cr systems the eutectic lines may not be entirely straight, but straight eutectic lines according to Fig. 1 are accurate enough for developing the model.

As it can be seen in Fig. 1, Al–Co–Ni, Al–Co–Cr and Al–Co–Fe eutectic lines origin from binary eutectic Al₂₀Co₈₀. For example, it can be said that Al–Co–Ni eutectics are formed by adding Ni to binary eutectic Al₂₀Co₈₀. Furthermore, it can be supposed that Al–Co–Cr and Al–Co–Fe eutectics are formed by adding respectively Cr and Fe to Al₂₀Co₈₀. So, it can be concluded that ternary eutectics Al–Co–Cr, Al–Co–Fe and Al–Co–Ni are

originated from binary eutectic Al₂₀Co₈₀. Similarly, one can assume that quaternary and quinary EHEAs are originated from binary eutectic Al₂₀Co₈₀. Furthermore, ternary eutectic compositions (all of the compositions on the eutectic lines in Fig. 1) can be considered as initial compositions for quaternary and quinary eutectic alloys. In general, it can be assumed that the quaternary and quinary eutectic alloys in Al–Co–Cr–Fe–Ni system are derived from binary and ternary eutectic alloys, and, as a result, it can be concluded that eutectic lines may exist between certain binary, ternary, quaternary and quinary eutectic alloys in Al–Co–Cr–Fe–Ni system. Based on this assumption, a network or graph structure can be proposed for eutectic alloys in Al–Co–Cr–Fe–Ni system. The proposed network or graph structure is schematically shown in Fig. 2. Each line which is shown in Fig. 2 is in fact showing a eutectic line which its existence can be verified by experiments or simulations. Therefore, some of the lines in Fig. 2 are shown by dashed lines meaning that their existence are not verified by experiments yet. The eutectic network which is shown in Fig. 2 could be used as a guideline for designing new eutectic alloys. The application of this network for designing new eutectic alloys is explained in next section. The eutectic network which is shown in Fig. 2 only contains a limited number of eutectic

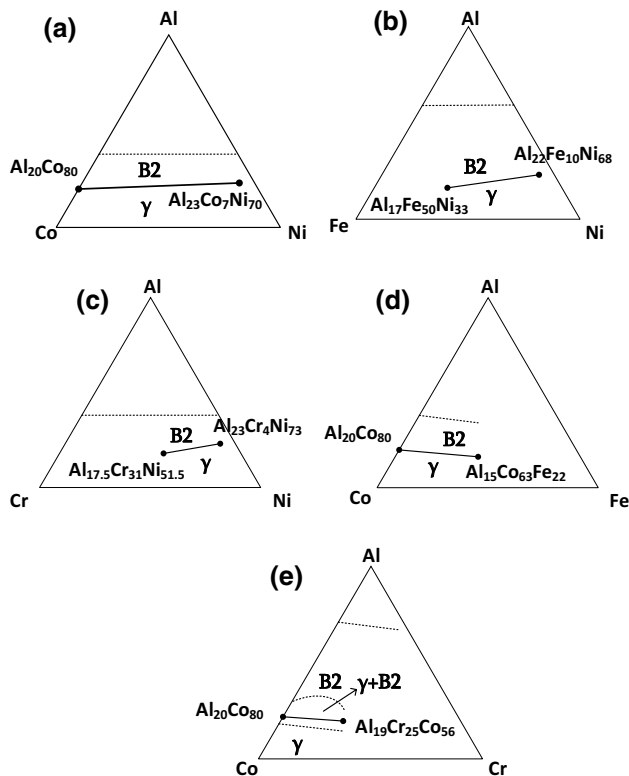


Fig. 1 The eutectic lines for **a** Al–Co–Ni [29, 30], **b** Al–Fe–Ni [26], **c** Al–Cr–Ni [27, 28], **d** Al–Co–Fe, and **e** Al–Co–Cr and systems. For Al–Co–Fe system the eutectic line is drawn between the minimum eutectic composition $Al_{15}Co_{63}Fe_{22}$ [31, 32] and eutectic composition $Al_{20}Co_{80}$ [33]. For Al–Co–Cr system the eutectic line is drawn according to the boundaries of $\gamma + B2$ region at 1300 °C [34]

alloys and can be expanded by considering all of the eutectic composition in Al–Co–Cr–Fe–Ni.

The concept of eutectic lines can also be explained by considering the phase rule. According to the phase rule ($F = C - P + 1$), a binary eutectic reaction (e. g. $L \rightarrow \gamma + B2$) has zero degree of freedom ($F = 2 - 3 + 1 = 0$) in a binary system. So this eutectic reaction is an invariant reaction in a binary phase diagram. In other words, a binary eutectic reaction can only occur at one temperature and composition

in a binary system. In a ternary system, F is equal to 1 ($F = 3 - 3 + 1 = 1$) for a binary eutectic reaction. As a result, there is a range of compositions for a binary eutectic reaction in a ternary system; this range is shown by a eutectic line on a ternary phase diagram (Fig. 1). Thus, a eutectic line on a ternary phase diagram is a set of eutectic compositions. In other words, each point on a eutectic line represents a eutectic composition. In a quinary system, F is equal to 3 ($F = 5 - 3 + 1 = 3$) for a binary eutectic reaction and it can be expected that the eutectic compositions form a volume within the phase diagram. As a result, eutectic lines can also be assumed for eutectic alloys in a quinary system. This is schematically shown in Fig. 3. Therefore, a eutectic line for a quinary system is a set of eutectic compositions within the eutectic volume of a quinary phase diagram. This concept is used in the present work, and it is shown that eutectic lines exist between certain eutectic alloys in Al–Co–Cr–Fe–Ni system; the compositions of experimentally verified eutectic alloys are used for finding these eutectic lines.

4 Designing New Eutectic Alloys

If a eutectic network similar to Fig. 2 can be developed for eutectic alloys in Al–Co–Cr–Fe–Ni system, then predicting new eutectic compositions will be very simple and straightforward. As an example, let’s assume that a eutectic line exists between eutectic compositions $Al_{20}Co_{80}$ [33] and $Al_{19.5}Co_{47.5}Cr_{7.5}Ni_{25.5}$ [12] (Fig. 4a). Therefore, the alloy $Al_{19.5}Co_{47.5}Cr_{7.5}Ni_{25.5}$ which is at the central point of the eutectic line may be eutectic as well. The simulation result for this alloy is shown in Fig. 4b which clearly shows that alloy $Al_{19.5}Co_{47.5}Cr_{7.5}Ni_{25.5}$ is eutectic. Furthermore, this alloy was made via casting and the optical images from the microstructure of alloy $Al_{19.5}Co_{47.5}Cr_{7.5}Ni_{25.5}$ are shown in Fig. 5. It can be seen that the microstructure of alloy $Al_{19.5}Co_{47.5}Cr_{7.5}Ni_{25.5}$ consists from a fine intimate mixture of two phases indicating that alloy $Al_{19.5}Co_{47.5}Cr_{7.5}Ni_{25.5}$ is eutectic. So the approach was successful in predicting a new eutectic alloy. A SEM image from the microstructure of

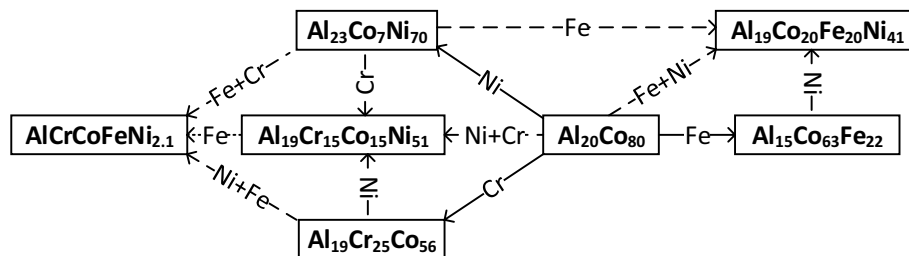


Fig. 2 Proposing a network or graph structure for some of the binary, ternary, quaternary and quinary eutectic alloys in Al–Co–Cr–Fe–Ni system; each line in the network represents a eutectic line and dashed

lines show eutectic lines which are not verified by experiments; as an example, the above network shows that eutectic $Al_{23}Co_{7}Ni_{70}$ is made by adding Ni to $Al_{20}Co_{80}$

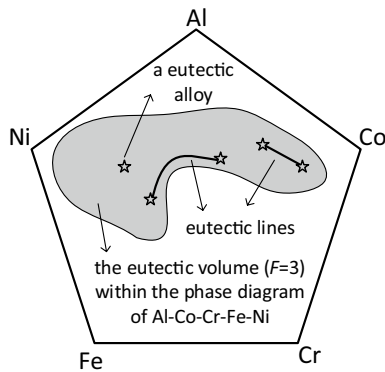


Fig. 3 The concept of eutectic lines between eutectic alloys in quinary Al–Co–Cr–Fe–Ni system

designed alloy is shown in Fig. 6. Energy Dispersive X-ray Analysis (EDX) was performed and the chemical composition was determined as $\text{Al}_{19.67}\text{Co}_{48.85}\text{Cr}_{7.94}\text{Ni}_{23.53}$ which is very close to the designed composition. According to Fig. 6, the inter-lamellar spacing is about $1\ \mu\text{m}$ which is half of the inter-lamellar spacing ($2\ \mu\text{m}$) reported for alloy $\text{AlCoCrFeNi}_{2.1}$ [6]. The hardness of alloy was measured to be $345 \pm 5\ \text{Hv}$.

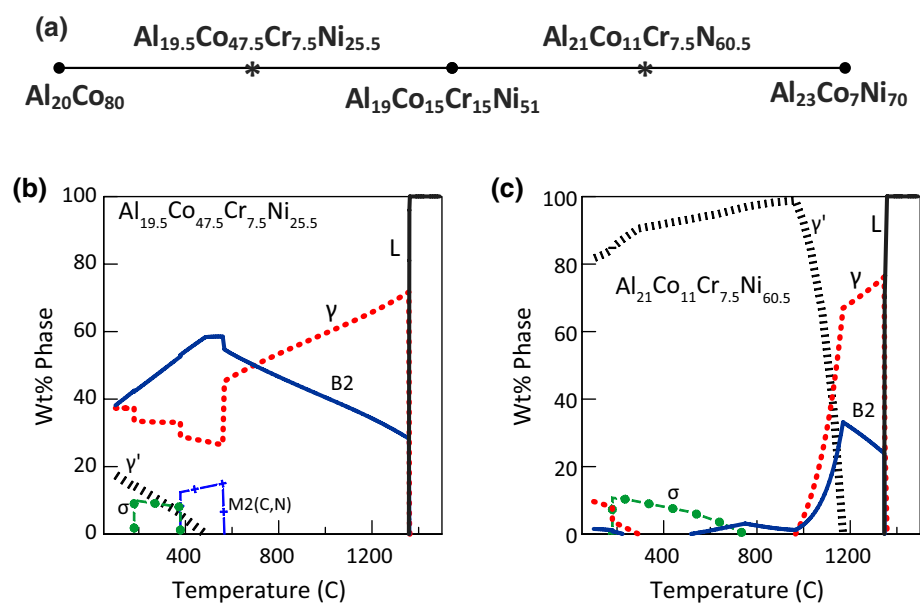
As another example, one can assume that a eutectic line exists between eutectic alloys $\text{Al}_{23}\text{Co}_7\text{Ni}_{70}$ [30] and $\text{Al}_{19}\text{Co}_{15}\text{Cr}_{15}\text{Ni}_{51}$ [12] (Fig. 4a). Therefore, the alloy $\text{Al}_{21}\text{Co}_{11}\text{Cr}_{7.5}\text{Ni}_{60.5}$ which is at the central point of the eutectic line may be eutectic as well. The simulation results for alloy $\text{Al}_{21}\text{Co}_{11}\text{Cr}_{7.5}\text{Ni}_{60.5}$ is shown in Fig. 4c which indicates that this alloy is eutectic. Therefore, it may be concluded that a eutectic line exists between two verified eutectic alloys $\text{Al}_{23}\text{Co}_7\text{Ni}_{70}$ [30] and $\text{Al}_{19}\text{Co}_{15}\text{Cr}_{15}\text{Ni}_{51}$ [12] and new

eutectic alloys can be designed by mixing the alloys at various molar ratios.

It should be noted that to accurately confirm that a eutectic line exists between two eutectic compositions, all of the alloy combinations (at 0.01:0.99 to 0.99:0.01 molar ratios) should be examined, and just examining the alloy at the central point may not be enough for confirming the existence of a eutectic line. But, examining all of the alloy combinations is very time consuming. Therefore, in the present work, three alloy combinations (alloys at 0.25:0.75, 1:1 and 0.75:0.25 molar ratios) are examined for investigating the existence of a eutectic line. If it can be shown that these three alloys are eutectic, then the chance for other alloys along that line to be eutectic is probably very high. So, in the present work it is assumed that if mixed alloys at 0.25:0.75, 1:1 and 0.75:0.25 molar ratio are eutectic, then there is a eutectic line between two eutectic alloys.

The results in Figs. 4 and 5 show that the assumption of the existence of eutectic lines between eutectic alloys is valid. To further examine this idea, more eutectic alloy combinations from Table 1 are examined by a procedure similar to Fig. 4, and three alloy combinations between two eutectic alloys (alloys at 0.25:0.75, 1:1 and 0.75:0.25 molar ratios) are examined. It is assumed that if alloys at 0.25:0.75, 1:1 and 0.75:0.25 molar ratios are eutectic, then there is a eutectic line between two eutectic alloys. The obtained simulation results are shown in Fig. 7 as a eutectic network. The narrow continuous lines show the eutectic lines which are verified by simulation results. The bold lines show eutectic lines which are verified by experiments (ternary eutectic lines in phase diagrams), and the dotted lines show lines which are examined by the software but are not eutectic according to simulation results. According to the proposed network in

Fig. 4 a Assuming eutectic lines between eutectic alloys $\text{Al}_{20}\text{Co}_{80}$ and $\text{Al}_{19}\text{Cr}_{15}\text{Co}_{15}\text{Ni}_{51}$ [12] and between $\text{Al}_{23}\text{Co}_7\text{Ni}_{70}$ [30] and $\text{Al}_{19}\text{Co}_{15}\text{Cr}_{15}\text{Ni}_{51}$ [12]; obtaining new eutectic alloys with compositions $\text{Al}_{19.5}\text{Co}_{47.5}\text{Cr}_{7.5}\text{Ni}_{25.5}$ and $\text{Al}_{21}\text{Co}_{11}\text{Cr}_{7.5}\text{Ni}_{60.5}$; the simulation results for alloys **b** $\text{Al}_{19.5}\text{Co}_{47.5}\text{Cr}_{7.5}\text{Ni}_{25.5}$ and **c** $\text{Al}_{21}\text{Co}_{11}\text{Cr}_{7.5}\text{Ni}_{60.5}$



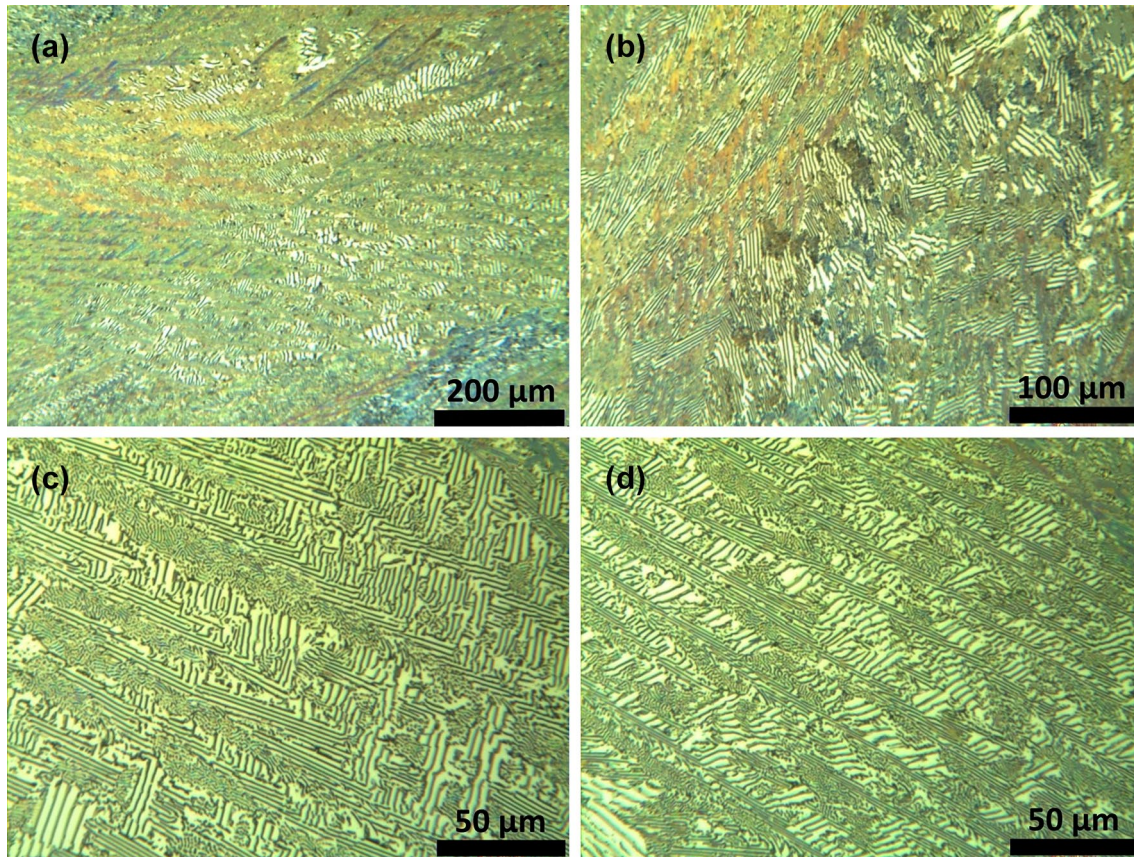


Fig. 5 a–d Optical images of the as-cast microstructure of alloy Al19.5Co47.5Cr7.5Ni25.5

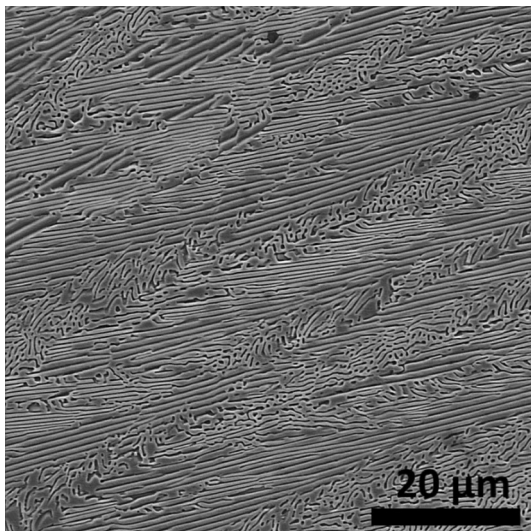


Fig. 6 A SEM image from the microstructure of alloy Al19.5Co47.5Cr7.5Ni25.5

Fig. 7, it can be seen that some of eutectic alloys are connected via eutectic lines meaning that those alloys may be mixed with each other for making other eutectic alloys. So, Fig. 7 provides a guideline for designing new eutectic alloy in Al–Co–Cr–Fe–Ni system. It should be noted that eutectic network which is shown in Fig. 7 is made by considering a limited number of eutectic alloy combinations. For making the complete eutectic network, all of the eutectic alloy combinations from Table 1 could be considered.

The dotted lines in Fig. 7 show lines which are examined by software but are not eutectic lines. It is observed that alloys along dotted lines are in fact near eutectic (hypo-eutectic or hyper-eutectic) alloys. Therefore, the alloys which are connected by dotted lines could be used for designing near eutectic (hypo-eutectic or hyper-eutectic) alloys. For example one can consider eutectic alloys $\text{Al}_{22}\text{Fe}_{10}\text{Ni}_{68}$ [26] and AlCrFeNi_2 ($\text{Al}_{16}\text{Cr}_{20}\text{Fe}_{20}\text{Ni}_{44}$) [35] which are connected by a dotted line according to Fig. 7. By mixing the alloys at 1:1 molar ratio, alloy $\text{Al}_{19}\text{Cr}_{10}\text{Fe}_{15}\text{Ni}_{56}$ can be obtained. The simulation results for alloy $\text{Al}_{19}\text{Cr}_{10}\text{Fe}_{15}\text{Ni}_{56}$ is shown in Fig. 8a which shows that this alloy is a near eutectic alloy because its solidification do not occur in a narrow range of temperature. Therefore, the alloys which are connected by

Fig. 7 The eutectic network obtained by considering some of the combinations of eutectic alloys in Table 1; the narrow eutectic lines are verified by simulation results, and the bold eutectic lines are verified by experiments, the dotted lines show the lines which are investigated but are not eutectic according to simulation results; the simulation results show that alloys along the dotted lines are in fact near eutectic alloys

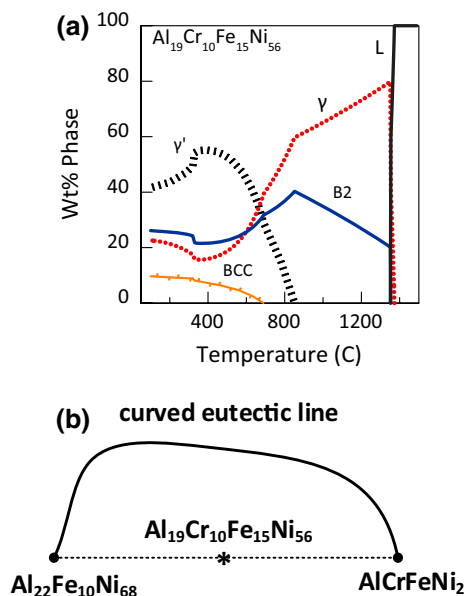
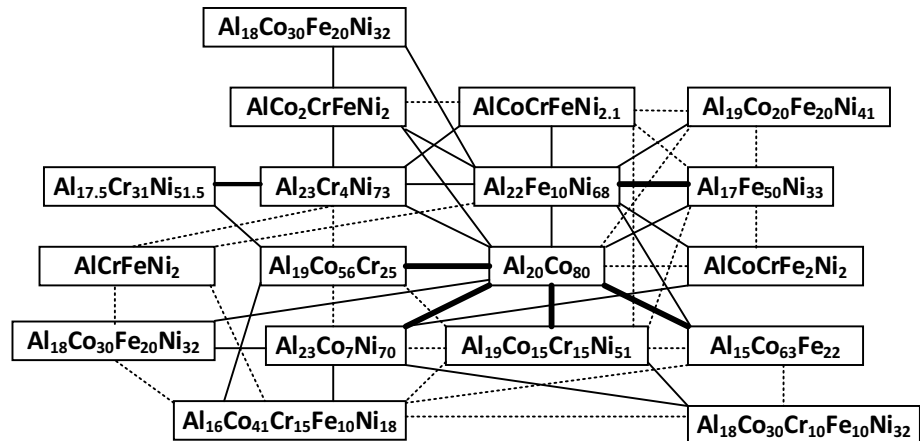


Fig. 8 **a** Simulation results for alloy $\text{Al}_{19}\text{Cr}_{10}\text{Fe}_{15}\text{Ni}_{56}$ obtained by mixing eutectic alloys $\text{Al}_{22}\text{Fe}_{10}\text{Ni}_{68}$ [26] and AlCrFeNi_2 [35], **b** assuming a curved eutectic line between alloys $\text{Al}_{22}\text{Fe}_{10}\text{Ni}_{68}$ [26] and AlCrFeNi_2 [35]; in this condition, alloys cannot be mixed with each other for designing new eutectic alloys

dotted lines can be used for obtaining near eutectic compositions. A curved eutectic line which is schematically shown in Fig. 8b can be assumed between alloys $\text{Al}_{22}\text{Fe}_{10}\text{Ni}_{68}$ [26] and AlCrFeNi_2 ($\text{Al}_{16}\text{Cr}_{20}\text{Fe}_{20}\text{Ni}_{44}$) [35]. According to Fig. 8b, when a curved eutectic line (where the eutectic compositions are arranged along a curve not a straight line) exists between two eutectic alloys, then the mixed alloys will not be located on the eutectic line. So the mixed alloys will not be eutectic.

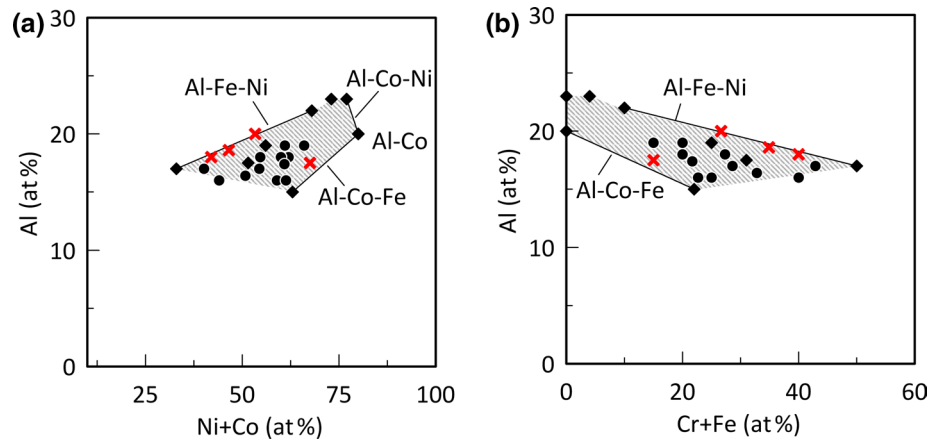
The eutectic network which is proposed in Fig. 7 is obtained only by thermodynamic simulations, and thermodynamic simulations are indeed used successfully by many research works for predicting the microstructures of alloys [38–43]. So the results in Fig. 7 may be valid and

applicable. Nevertheless, the most reliable way for examining the existence of eutectic lines between eutectic compositions is performing the experiments. So experiments are needed for accurately confirming the eutectic network in Fig. 7. In the present work, just one eutectic composition ($\text{Al}_{19.5}\text{Co}_{47.5}\text{Cr}_{7.5}\text{Ni}_{25.5}$) at the central point between alloys $\text{Al}_{20}\text{Co}_{80}$ [33] and $\text{Al}_{19}\text{Co}_{15}\text{Cr}_{15}\text{Ni}_{51}$ [12] is confirmed, but it is believed that more eutectic alloys could be obtained by using a similar approach. In the following section some compositional diagrams are proposed for evaluating the composition of EHEAs in Al–Co–Cr–Fe–Ni system. They could be used alongside with the developed method for evaluating the composition of EHEAs in Al–Co–Cr–Fe–Ni system.

5 Compositional Diagrams

Because it is proposed that EHEAs are derived from binary and ternary eutectic compositions, therefore it can be expected that the concentration of elements in EHEAs should be within specific ranges. For example, according to Table 1, the Al concentration of binary and ternary eutectic alloys is in the range of 15–23 at%. Therefore, the Al concentration of EHEAs should be within this range as well. As it can be seen, the Al concentration of EHEAs (Table 1) is indeed within this range. The Al concentration of EHEAs alloys can also be investigated by Fig. 9a, b. Figure 9a shows the Al concentration versus (Ni + Co) concentration, and Fig. 9b shows the Al concentration versus (Cr + Fe) concentration of all eutectic alloys in Table 1. By considering the relation $\text{Al} + \text{Co} + \text{Cr} + \text{Fe} + \text{Ni} = 100$, these two diagrams have the same meaning; but both diagrams are plotted so the relations could be more easily understood. It can be seen that there are regions limited by binary and ternary eutectics in which all EHEAs are located. This observation suggests that EHEAs are all originated from binary and ternary eutectic alloys. Furthermore, it can be postulated that all EHEAs in Al–Co–Cr–Fe–Ni system should be located within eutectic

Fig. 9 The Al concentration versus **a** (Ni + Co) and **b** (Cr + Fe) concentration of binary and ternary (filled diamond) and quaternary and quinary (filled circle) eutectic alloys in Table 1; four not-eutectic alloys are shown by (×)



regions in Fig. 9. Moreover, it can be proposed that if the Al concentration of an alloy is not within the eutectic regions in Fig. 9, then that alloy cannot be eutectic. So eutectic regions in Fig. 9 provide references for evaluating the Al concentration of EHEAs.

It should be noted that every alloy which can be located inside of the eutectic regions in Fig. 9 is not necessarily eutectic. To clarify this point, not-eutectic alloys in Table 2 can be considered. Most of the alloys in Table 2 will be located outside of the eutectic regions in Fig. 9 (the results are not shown in Fig. 9 for clarity of the diagrams), but four near-eutectic alloys $\text{Al}_{17}\text{Co}_{15}\text{Cr}_{15}\text{Ni}_{52.5}$ [12], $\text{Al}_{0.75}\text{CoFeNi}$ [35], $\text{Al}_{0.9}\text{CrFeNi}_{2.1}$ [35] and $\text{Al}_{0.8}\text{CoCr}_{0.5}\text{FeNi}$ [55] will be located within the eutectic regions close to the Al–Fe–Ni and Al–Co–Ni eutectic lines. These four not-eutectic alloys are shown in Fig. 9 by crosses. Therefore, it can be concluded that every alloy which is located inside of the eutectic regions in Fig. 9 is not necessarily eutectic. Eutectic regions in Fig. 9 just defines the limits for the Al, (Ni + Co) and (Cr + Fe) concentrations of EHEAs.

Figure 10a shows the Cr concentration versus (Co + Ni + Fe) concentration and Fig. 10b shows the Fe concentration versus (Co + Ni + Cr) concentration of eutectic alloys in Table 1. It can be seen that the maximum concentration of Cr in eutectic alloys is 31 at% which belongs to ternary eutectic alloy $\text{Al}_{17.5}\text{Cr}_{31}\text{Ni}_{51.5}$ [27, 28]. Therefore, it can be predicted that the Cr concentration of EHEAs should be less than 31 at%. According to Table 1 it can be seen that the Cr concentration of EHEAs is indeed less than 31 at%. According to the diagrams in Fig. 10, it can be seen that there are narrow regions limited by binary and ternary eutectic compositions in which all EHEAs are located suggesting that EHEAs are all originated from binary and ternary eutectic alloys. Furthermore, it can be anticipated that the Cr and Fe concentration of all (γ + B2) EHEAs in Al–Co–Cr–Fe–Ni system should be within the eutectic regions which are shown in Fig. 10. Therefore, eutectic regions in Fig. 10 can be used as references for

checking the Cr and Fe concentrations of (γ + B2) EHEAs in Al–Co–Cr–Fe–Ni system. As it is shown in Fig. 10, four near-eutectic alloys $\text{Al}_{17}\text{Co}_{15}\text{Cr}_{15}\text{Ni}_{52.5}$ [12], $\text{Al}_{0.75}\text{CoFeNi}$ [35], $\text{Al}_{0.9}\text{CrFeNi}_{2.1}$ [35] and $\text{Al}_{0.8}\text{CoCr}_{0.5}\text{FeNi}$ [55] are located within the eutectic regions in Fig. 10. This indicates that every alloy which can be located inside of the eutectic regions in Fig. 10 is not necessarily eutectic.

Similar to diagrams in Figs. 9 and 10, compositional diagrams of (Co + Ni) versus (Cr + Fe) and (Co + Cr) versus (Fe + Ni) can be considered for evaluating the composition of eutectic alloys in Al–Co–Cr–Fe–Ni system as they are shown in Fig. 11a, b. According to these compositional diagrams, again narrow regions between binary and ternary eutectic alloys can be defined within which all EHEAs are located. Therefore, it may be speculated that all EHEAs should be within the narrow regions in Fig. 11a, b. By considering the relation ($\text{Al} + \text{Co} + \text{Cr} + \text{Fe} + \text{Ni} = 100$), diagrams in Fig. 11a, b can also be used for evaluating the Al concentration of EHEAs.

Another diagram for examining the compositions of EHEAs can be $\text{Al}/(\text{Co} + \text{Ni})$ versus $\text{Al}/(\text{Cr} + \text{Fe})$ which simultaneously considers the five constituent elements. This diagram is shown in Fig. 11c. According to this figure, a region which is limited by binary and ternary eutectic compositions can be defined in which all EHEAs are located. The diagrams in Fig. 11 may be used in alongside with diagrams in Figs. 9, 10 for evaluating the composition of EHEAs. According to the diagrams in Fig. 11, it can be seen that four near-eutectic alloys $\text{Al}_{17}\text{Co}_{15}\text{Cr}_{15}\text{Ni}_{52.5}$ [12], $\text{Al}_{0.75}\text{CoFeNi}$ [35], $\text{Al}_{0.9}\text{CrFeNi}_{2.1}$ [35] and $\text{Al}_{0.8}\text{CoCr}_{0.5}\text{FeNi}$ [55] are located within the eutectic regions or near the eutectic region boundaries. Therefore, it can be concluded that every alloy which is located inside of the eutectic regions in Fig. 11 is not necessarily eutectic. Diagrams in Fig. 11 just define concentration limits for the constituent elements of EHEAs.

Diagrams in Figs. 9, 10, 11 are in fact two dimensional projections of some parts of the quinary phase

Table 2 Chemical compositions of some of the experimentally verified not-eutectic alloys in Al–Co–Cr–Fe–Ni system

Alloys	Chemical composition (at%)					Phases in as cast structure
	Al	Co	Cr	Fe	Ni	
Al _x CoCrFeNi [44, 45]	0	25	25	25	25	γ (FCC)
Al _x CoCrFeNi [44, 45]	6	23.5	23.5	23.5	23.5	γ+B2 (BCC)
Al _x CoCrFeNi [44, 45]	11	22.25	22.25	22.25	22.25	γ+B2
Al _x CoCrFeNi [44, 45]	15	21.25	21.25	21.25	21.25	γ+B2
Al _x CoCrFeNi [44, 45]	20	20	20	20	20	α (BCC)+B2
Fe ₃₄ Cr ₃₄ Ni ₁₄ Al ₁₄ Co ₄ [46]	14	4	34	34	14	α+B2
Al _{0.7} NiCoFeCr ₂ [47]	12.5	17.5	35	17.5	17.5	α+B2
Al _{1.3} CrFeNi [48]	30	0	23.33	23.33	23.34	α+B2
Al _{12.5} Ni ₂₅ Co ₂₅ Fe _{18.75} Cr _{18.75} [49]	12.5	25	18.75	18.75	25	γ+B2
Al _{12.5} Ni _{17.5} Co _{17.5} Fe ₃₅ Cr _{17.5} [49]	12.5	17.5	17.5	35	17.5	α+γ+B2
Al ₂ (NiCoFeCr) ₁₄ [50]	12.5	21.875	21.875	21.875	21.875	α+γ+B2
Al ₂ (Ni ₄ Co ₄ Fe ₃ Cr ₃) ₁₄ [50]	12.5	25	18.75	18.75	25	γ+α+B2
Al ₂ (NiCoFe ₂ Cr) ₁₄ [50]	12.5	17.5	17.5	35	17.5	γ+α+B2
Al ₂ (NiCoFeCr ₂) ₁₄ [50]	12.5	17.5	35	17.5	17.5	γ+α+B2
Al _{0.7} NiCoFe _{1.5} Cr _{1.5} [51]	12.3	17.5	26.35	26.35	17.5	α+B2
Al _x Co ₁₅ Cr ₁₅ Ni _{70-x} [12]	5	15	15	0	65	γ
Al _x Co ₁₅ Cr ₁₅ Ni _{70-x} [12]	12.5	15	15	0	57.5	γ+L ₁₂
Al _x Co ₁₅ Cr ₁₅ Ni _{70-x} [12]	17.5	15	15	0	52.5	γ+L ₁₂ +B2
Al _x Co ₁₅ Cr ₁₅ Ni _{70-x} [12]	27.5	15	15	0	42.5	γ+B2
Al _x Co ₁₅ Cr ₁₅ Ni _{70-x} [12]	35	15	15	0	35	B2
Al _{0.6} CoCrFeNi [52]	13	21.75	21.75	21.75	21.75	γ+B2
Al _x Co _{2-x} CrFeNi [53]	5	35	20	20	20	γ
Al _x Co _{2-x} CrFeNi [53]	10	30	20	20	20	γ+B2
Al _x Co _{2-x} CrFeNi [53]	15	25	20	20	20	γ+B2
Al _x Co _{2-x} CrFeNi [53]	20	20	20	20	20	B2
Al _x Co _{2-x} CrFeNi [53]	25	15	20	20	20	B2
Al _x Co _{2-x} CrFeNi [53]	30	10	20	20	20	B2
Al _x Co _{2-x} CrFeNi [53]	35	5	20	20	20	B2
Al _x CoFeNi [54]	0	33.33	0	33.33	33.34	γ
Al _x CoFeNi [54]	7.7	30.7	0	30.7	30.9	γ
Al _x CoFeNi [54]	14.2	28.6	0	28.6	28.6	γ+B2
Al _x CoFeNi [54]	20	26.65	0	26.65	26.7	γ+B2
Al _x CoFeNi [54]	25	25	0	25	25	B2
Al _x CrFeNi _{3-x} [35]	20	0	20	20	40	γ+B2
Al _x CrFeNi _{3-x} [35]	18	0	20	20	42	γ+B2
Al _x CrFeNi _{3-x} [35]	14	0	20	20	46	γ+B2
Al _x CrFeNi _{3-x} [35]	12	0	20	20	48	γ+B3
Al _x CoCr _{0.5} FeNi [55]	14.6	24.4	12.2	24.4	24.4	γ+B2
Al _x CoCr _{0.5} FeNi [55]	18.6	23.26	11.63	23.25	23.26	γ+B2
Al _x CoCr _{0.5} FeNi [55]	22.23	22.22	11.11	22.22	22.22	γ+B2
Al _x CoCr _{0.5} FeNi [55]	25.53	21.28	10.63	21.28	21.28	γ+B2

diagram Al–Co–Cr–Fe–Ni. Therefore, they cannot exactly define the eutectic volume in the quinary phase diagram Al–Co–Cr–Fe–Ni. That is why some not-eutectic alloys are also located inside of the eutectic regions in Figs. 9, 10, 11. The diagrams in Figs. 9, 10, 11 can only be used for evaluating the composition of EHEAs because they define the limits for the concentration of constituent elements in EHEAs.

The composition of new EHEAs cannot be extracted from eutectic regions in Figs. 9, 10, 11. That is because not-eutectic alloys may also be located inside eutectic regions in Figs. 9, 10, 11. If someone wants to use these diagrams for extracting the composition of new EHEAs, then the boundaries of eutectic regions in Figs. 9, 10, 11 should be defined more accurately which needs more

Fig. 10 **a** The Cr concentration versus (Ni+Co+Fe) concentration and **b** the Fe concentration versus (Ni+Co+Cr) concentration of binary and ternary (filled diamond) and quaternary and quinary (filled circle) eutectic alloys in Table 1; four not-eutectic alloys are shown by (×)

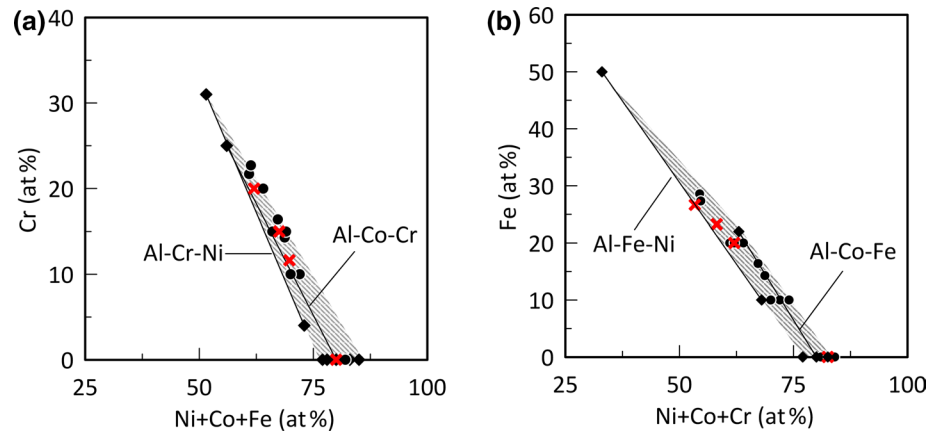
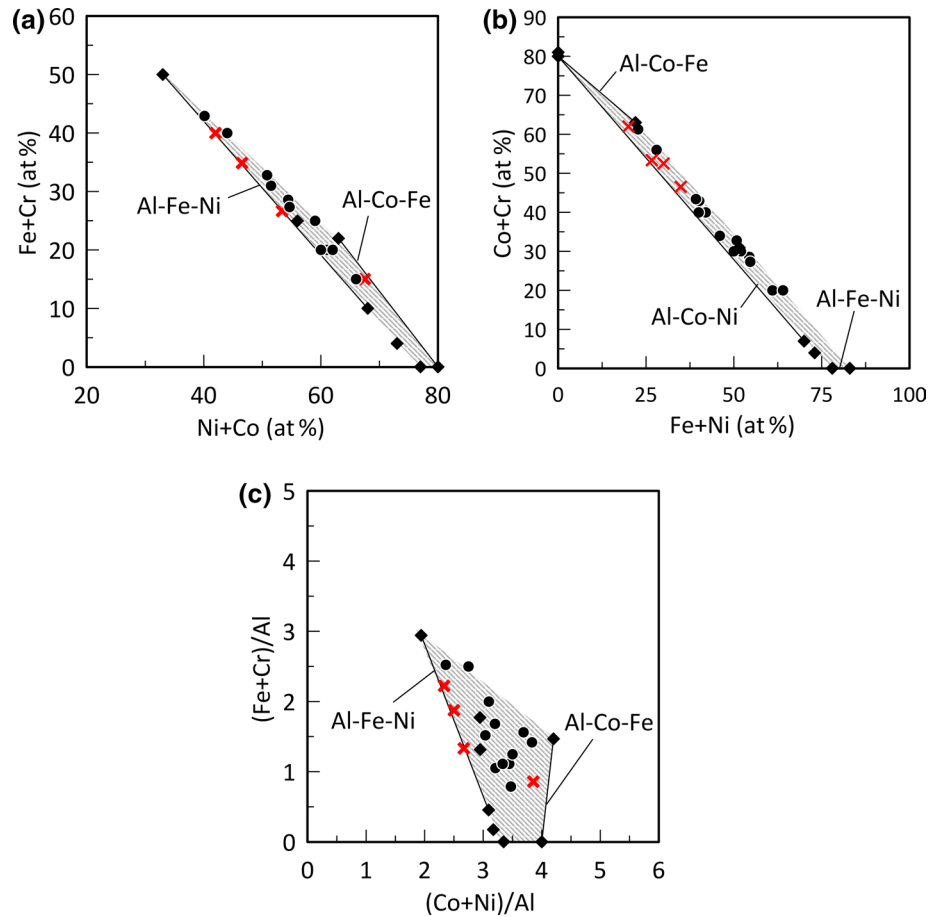


Fig. 11 **a** (Co+Ni) versus (Cr+Fe), **b** (Co+Cr) versus (Ni+Fe) and **c** (Fe+Cr)/Al versus (Co+Ni)/Al for binary and ternary (filled diamond), and quaternary and quinary (filled circle) eutectic alloys in Table 1; four not-eutectic alloys are shown by (×)



experimental data. Furthermore, all of the diagrams in Figs. 9, 10, 11 must be used simultaneously for designing new eutectic alloys. In other words, to design a new EHEA, the composition of the alloy should be checked against all of the diagrams in Figs. 9, 10, 11 and all of the diagrams must indicate that the alloy is in eutectic regions. Furthermore, other compositional diagrams maybe developed by which eutectic and not-eutectic alloys can be categorized more accurately. If such diagrams can

be developed, then they can be used for predicting the composition of EHEAs.

According to the diagrams in Figs. 9, 10, 11, it can be seen that ranges of concentration exist for each constituent element of EHEAs in Al–Co–Cr–Fe–Ni system. Therefore, it can be concluded that a great number of $\gamma + B2$ eutectic alloys exist in Al–Co–Cr–Fe–Ni system. Up to now, only a limited number of eutectic alloys are reported, but further eutectic alloys with excellent properties may be expected.

The approach which is presented in the present work proposes a simple method for designing new eutectic alloys, and the obtained compositional diagrams present references for evaluating the composition of eutectic alloys.

6 Conclusions

1. A new approach is presented for designing new eutectic high entropy alloys (EHEAs) in Al–Co–Cr–Fe–Ni system by introducing the concept of eutectic lines. It is proposed that eutectic lines exist between certain eutectic alloys in Al–Co–Cr–Fe–Ni system. As a result, new eutectic alloys can be designed by mixing the eutectic alloys which are located on the same eutectic line. By applying the proposed approach, new eutectic or near eutectic alloys are designed for Al–Co–Cr–Fe–Ni system.
2. Based on the concept of eutectic lines, a network or graph structure is proposed for eutectic alloys in Al–Co–Cr–Fe–Ni system in which the eutectic alloys which are connected via eutectic lines are determined. The proposed network can be used as a guideline for designing new eutectic alloy in Al–Co–Cr–Fe–Ni system.
3. By investigating the compositions of verified eutectic alloys in Al–Co–Cr–Fe–Ni system, compositional diagrams are proposed which show the relations between the concentrations of constituent elements in EHEAs. The proposed diagrams can be considered as convenient methods for evaluating the composition of EHEAs.

Acknowledgements This research was supported by Niroo Research Institute (NRI) [Grant Numbers 22122 & 380115]. I thank Dr. Reza Gholamipour with the Department of Advanced Materials and Renewable Energy, Iranian Research Organization for Science and Technology (IROST) for sample preparation.

References

1. E.P. George, D. Raabe, R.O. Ritchie, High-entropy alloys. *Nat. Rev. Mater.* **4**, 515 (2019)
2. D.B. Miracle, High entropy alloys as a bold step forward in alloy development. *Nat. Commun.* **10**, 1805 (2019)
3. D.B. Miracle, O.N. Senkov, A critical review of high entropy alloys and related concepts. *Acta Mater.* **122**, 448 (2017)
4. Y. Zhang, T.T. Zuo, Z. Tang, M.C. Gao, K.A. Dahmen, P.K. Liaw, Z.P. Lu, Microstructures and properties of high-entropy alloys. *Prog. Mater. Sci.* **61**, 1 (2014)
5. Y.F. Ye, Q. Wang, J. Lu, C.T. Liu, Y. Yang, High-entropy alloy: challenges and prospects. *Mater. Today* **19**, 349 (2016)
6. Y. Lu, Y. Dong, S. Guo, L. Jiang, H. Kang, T. Wang, B. Wen, Z. Wang, J. Jie, Z. Cao, H. Ruan, T. Li, A promising new class of high-temperature alloys: eutectic high-entropy alloys. *Sci. Rep.* **4**, 6200 (2014)
7. X. Gao, Y. Lu, B. Zhang, N. Liang, G. Wu, G. Sha, J. Liu, Y. Zhao, Microstructural origins of high strength and high ductility in an AlCoCrFeNi_{2.1} eutectic high-entropy alloy. *Acta Mater.* **141**, 59 (2017)
8. I.S. Wani, T. Bhattacharjee, S. Sheikh, P.P. Bhattacharjee, S. Guo, N. Tsuji, Tailoring nanostructures and mechanical properties of AlCoCrFeNi_{2.1} eutectic high entropy alloy using thermo-mechanical processing. *Mater. Sci. Eng. A* **675**, 99 (2016)
9. F. He, Z. Wang, P. Cheng, Q. Wang, J. Li, Y. Dang, J. Wang, C.T. Liu, Designing eutectic high entropy alloys of CoCrFeNiNb_x. *J. Alloys Compd.* **656**, 284 (2016)
10. Y. Lu, X. Gao, L. Jiang, Z. Chen, T. Wang, J. Jie, H. Kang, Y. Zhang, S. Guo, H. Ruan, Y. Zhao, Z. Cao, T. Li, Directly cast bulk eutectic and near-eutectic high entropy alloys with balanced strength and ductility in a wide temperature range. *Acta Mater.* **124**, 143 (2017)
11. I. Baker, M. Wu, Z. Wang, Eutectic/eutectoid multi-principle component alloys: a review. *Mater. Charact.* **147**, 545 (2019)
12. D. Liu, P. Yu, G. Li, P.K. Liaw, R. Liu, High-temperature high-entropy alloys Al_xCo₁₅Cr₁₅Ni_{70-x} based on the Al–Ni binary system. *Mater. Sci. Eng. A* **724**, 283 (2018)
13. X. Jin, Y. Zhou, L. Zhang, X. Du, B. Li, A novel Fe₂₀Co₂₀Ni₄₁Al₁₉ eutectic high entropy alloy with excellent tensile properties. *Mater. Lett.* **216**, 144 (2018)
14. M. Wu, S. Wang, H. Huang, D. Shu, B. Sun, CALPHAD aided eutectic high-entropy alloy design. *Mater. Lett.* **262**, 127175 (2020)
15. A. Patel, I. Wani, S.R. Reddy, S. Narayanaswamy, A. Lozinko, R. Saha, S. Guo, P.P. Bhattacharjee, Strain-path controlled microstructure, texture and hardness evolution in cryo-deformed AlCoCrFeNi_{2.1} eutectic high entropy alloy. *Intermetallics* **97**, 12 (2018)
16. Y. Lu, H. Jiang, S. Guo, T. Wang, Z. Cao, T. Li, A new strategy to design eutectic high-entropy alloys using mixing enthalpy. *Intermetallics* **91**, 124 (2017)
17. H. Jiang, K. Han, X. Gao, Y. Lu, Z. Cao, M.C. Gao, J.A. Hawk, T. Li, A new strategy to design eutectic high-entropy alloys using simple mixture method. *Mater. Des.* **142**, 101 (2018)
18. X. Jin, Y. Zhou, L. Zhang, X. Du, B. Li, A new pseudo binary strategy to design eutectic high entropy alloys using mixing enthalpy and valence electron concentration. *Mater. Des.* **143**, 49 (2018)
19. JMatPro (Java-based Materials Property simulation software, version 7.0.0), Sente Software Ltd., Surrey Technology Center, 40 Occam Road, Guildford, Surrey GU2 7YG, UK
20. N. D'Souza, H.B. Dong, Solidification path in third-generation Ni-based superalloys with an emphasis on last stage solidification. *Scr. Mater.* **56**, 41 (2007)
21. N. Saunders, U.K.Z. Guo, X. Li, A.P. Miodownik, JPh Schillé, Using JMatPro to model materials properties and behavior. *JOM* **55**, 60 (2003)
22. Z. Guo, N. Saunders, A.P. Miodownik, J. Ph. Schille: Modelling of materials properties and behaviour critical to casting simulation. *Mater. Sci. Eng. A* **413**, 465 (2005)
23. N. D'Souza, M. Lekstrom, H.B. Dong, An analysis of measurement of solute segregation in Ni-base superalloys using X-ray spectroscopy. *Mat. Sci. Eng. A* **460**, 258 (2008)
24. Z. Guo, N. Saunders, J.P. Schillé, A.P. Miodownik, Material properties for process simulation. *Mater. Sci. Eng. A* **499**, 7 (2009)
25. A. Shafiei, S. Rajabi, A cobalt-rich eutectic high-entropy alloy in the system Al–Co–Cr–Fe–Ni. *Appl. Phys. A* **125**, 783 (2019)
26. L. Zhang, Y. Du, Thermodynamic description of the Al–Fe–Ni system over the whole composition and temperature ranges: Modeling coupled with key experiment. *Calphad* **31**, 529 (2007)
27. N. Dupin, I. Ansara, B. Sundman, Thermodynamic re-assessment of the ternary system Al–Cr–Ni. *Calphad* **25**, 279 (2001)

28. Y. Wang, G. Cacciamani, Thermodynamic modeling of the Al–Cr–Ni system over the entire composition and temperature range. *J. Alloys Compd.* **688**, 422 (2016)
29. G. Effenberg and S. Ilyenko (Eds.): *Light Metal Systems. Part 1: Selected Systems from Ag–Al–Cu to Al–Cu–Er* (Springer, Berlin, 2004), pp. 246, 288
30. Y. Wang, G. Cacciamani, Experimental investigation and thermodynamic assessment of the Al–Co–Ni system. *Calphad* **61**, 198 (2018)
31. L. Zhu, S. Soto-Medina, R.G. Hennig, M.V. Manuel, Experimental investigation of the Al–Co–Fe phase diagram over the whole composition range. *J. Alloys Compd.* **815**, 152110 (2020)
32. G. Effenberg and S. Ilyenko (Eds.): *Light Metal Systems. Part 1: Selected Systems from Ag–Al–Cu to Al–Cu–Er* (Springer, Berlin, 2004), pp. 206, 216
33. H. Baker (ed.), *ASM Handbook, Alloy Phase Diagrams* (ASM International, Materials Park, Ohio, 1992)
34. X.L. Liu, G. Lindwall, T. Gheno, Z.K. Liu, Thermodynamic modeling of Al–Co–Cr, Al–Co–Ni, Co–Cr–Ni ternary systems towards a description for Al–Co–Cr–Ni. *Calphad* **52**, 125 (2016)
35. X. Jin, J. Bi, L. Zhang, Y. Zhou, X. Du, Y. Liang, B. Li, A new CrFeNi₂Al eutectic high entropy alloy system with excellent mechanical properties. *J. Alloys Compd.* **770**, 655 (2019)
36. Z. Yang, Z. Wang, Q. Wu, T. Zheng, P. Zhao, J. Zhao, J. Chen, Enhancing the mechanical properties of casting eutectic high entropy alloys with Mo addition. *Appl. Phys. A* **125**, 208 (2019)
37. Q. Wu, Z. Wang, X. Hu, T. Zheng, Z. Yang, F. He, J. Li, J. Wang, Uncovering the eutectics design by machine learning in the Al–Co–Cr–Fe–Ni high entropy system. *Acta Mater.* **182**, 278 (2020)
38. M.C. Gao, J. W. Yeh, P.K. Liaw, Y. Zhang (editors): *High-entropy alloys: fundamentals and applications*, 1st ed. (Springer, Cham, Switzerland, 2016), pp. 399, 444.
39. C. Zhang, F. Zhang, S. Chen, W. Cao, Computational thermodynamics aided high-entropy alloy design. *JOM* **64**, 839 (2012)
40. F. Zhang, C. Zhang, S.L. Chen, J. Zhu, W.S. Cao, U.R. Kattner, An understanding of high entropy alloys from phase diagram calculations. *Calphad* **45**, 1 (2014)
41. O.N. Senkov, J.D. Miller, D.B. Miracle, C. Woodward, Accelerated exploration of multi-principal element alloys for structural applications. *Calphad* **50**, 32 (2015)
42. C. Zhang, F. Zhang, H. Diao, M.C. Gao, Z. Tang, P.K. Liaw, Understanding phase stability of Al–Co–Cr–Fe–Ni high entropy alloys. *Mater. Des.* **109**, 425 (2016)
43. M.C. Gao, C. Zhang, P. Gao, F. Zhang, L.Z. Ouyang, M. Widom, J.A. Hawk, Thermodynamics of concentrated solid solution alloys. *Curr. Opin. Solid State Mater. Sci.* **21**, 238 (2017)
44. T. Yang, S. Xia, S. Liu, C. Wang, S. Liu, Y. Zhang, J. Xue, S. Yan, Y. Wang, Effects of AL addition on microstructure and mechanical properties of Al_xCoCrFeNi high entropy alloy. *Mater. Sci. Eng. A* **648**, 15 (2015)
45. W.R. Wang, W.L. Wang, S.C. Wang, Y.C. Tsai, C.H. Lai, J.W. Yeh, Effects of Al addition on the microstructure and mechanical property of Al_xCoCrFeNi high-entropy alloys. *Intermetallics* **26**, 44 (2012)
46. Y. Zhou, X. Jin, L. Zhang, X. Du, B. Li, A hierarchical nanostructured Fe₃₄Cr₃₄Ni₁₄Al₁₄Co₄ high-entropy alloy with good compressive mechanical properties. *Mater. Sci. Eng. A* **716**, 235 (2018)
47. C. Li, Y. Ma, J. Hao, Q. Wang, S. Pang, C. Dong, P.K. Liaw, Effect of Ti substitution for Al on the cuboidal nanoprecipitates in Al_{0.7}NiCoFeCr₂ high-entropy alloys. *J. Mater. Res.* **33**, 3266 (2018)
48. X. Chen, Y. Sui, J. Qi, Y. He, F. Wei, Q. Meng, Z. Sun, Microstructure of Al_{1.3}CrFeNi eutectic high entropy alloy and oxidation behavior at 1000 °C. *J. Mater. Res.* **32**, 2109 (2017)
49. Y. Ma, Q. Wang, C. Li, L.J. Santodonato, M. Feygenson, C. Dong, P.K. Liaw, Chemical short-range orders and the induced structural transition in high-entropy alloys. *Scr. Mater.* **144**, 64 (2018)
50. Y. Ma, Q. Wang, B.B. Jiang, C.L. Li, J.M. Hao, X.N. Li, C. Dong, T.G. Nieh, Controlled formation of coherent cuboidal nanoprecipitates in body-centered cubic high-entropy alloys based on Al₂(Ni Co, Fe, Cr)₁₄ compositions. *Acta Mater.* **147**, 213 (2018)
51. J. Hao, Y. Ma, Q. Wang, C. Zhang, C. Li, C. Dong, Q. Song, P.K. Liaw, Formation of cuboidal B2 nanoprecipitates and microstructural evolution in the body-centered-cubic Al_{0.7}NiCoFe_{1.5}Cr_{1.5} high-entropy. *J. Alloys Compd.* **780**, 408 (2019)
52. M. Chen, L. Lan, X. Shi, H. Yang, M. Zhang, J. Qiao, The tribological properties of Al_{0.6}CoCrFeNi high-entropy alloy with the σ phase precipitation at elevated temperature. *J. Alloys Compd.* **777**, 180 (2019)
53. Y. Sun, C. Wu, H. Peng, Y. Liu, J. Wang, X. Su, Phase constituent and microhardness of as-cast and long-time annealed Al_xCo_{2-x}CrFeNi multicomponent alloys. *J. Phase Equilibria Diffus.* **40**, 706 (2019)
54. T.T. Zuo, R.B. Li, X.J. Ren, Y. Zhang, Effects of Al and Si addition on the structure and properties of CoFeNi equal atomic ratio alloy. *J. Magn. Magn. Mater.* **371**, 60 (2014)
55. T. Lu, W. Chai, T. Dai, Y. Pan, FeCoNiCr_{0.5}Al_x high-entropy alloys with dual-phase solidification microstructure and high compressive properties. *JOM* **71**, 3460 (2019)

Publisher's Note Springer Nature remains neutral with regard to jurisdictional claims in published maps and institutional affiliations.